Ecological Indicators 128 (2021) 107798

Contents lists available at ScienceDirect

Ecological Indicators

journal homepage: www.elsevier.com/locate/ecolind

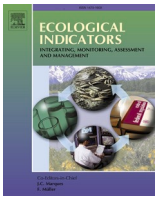

Will climate change shift carbon allocation and stem hydraulics? Insights on a systemic view of carbon- and water-related wood traits in an anysohydric tropical tree species (*Hymenaea courbaril*, Leguminosae)

Bernardo Pretti Becacici Macieira [a,b,1], Giuliano Maselli Locosselli [c,d,1,*], Marcos Silveira Buckeridge [c], Vinícius Carvalho Jardim [e], Stefan Krottenthaler [f], Dieter Anhuf [f], Gerhard Helle [g], Geraldo Rogério Faustini Cuzzuol [a], Gregório Ceccantini [a]

[a] Department of Forest and Wood Sciences, Federal University of Espírito Santo, 29550-000 Jerônimo Monteiro, Brazil
[b] Department of Biological Sciences, Federal University of Espírito Santo, 29075-910 Vitória, Brazil
[c] Department of Botany, Institute of Biosciences, University of São Paulo, 05508-090 São Paulo, Brazil
[d] Institute of Botany, Cluster of Ecology, 04301-902 São Paulo, Brazil
[e] Department of Computer Science, Institute of Mathematics and Statistics, University of São Paulo, 05508-090 São Paulo, Brazil
[f] Department of Physical Geography, University of Passau, Innstraße 40, 94032 Passau, Germany
[g] German Research Centre for Geosciences—GFZ, Section 5.2 Climate Dynamics and Landscape Evolution, Potsdam Dendro Laboratory, Telegrafenberg, 14473 Potsdam, Germany

ARTICLE INFO

Keywords:
Tree rings
Dendrobiochemistry
Carbon allocation
Vessel features
Carbon isotopes
Complex networks

ABSTRACT

Tropical forests uptake more atmospheric CO_2 and transpire more water than any other forest in the world and are critical components of the global carbon and hydrological cycles. Both cycles depend to a great extent on the carbon and water balance of individual trees. Such adjustments are usually evaluated through well-established and newly-emerging traits but integrating them for a systemic understanding of trees' responses to climate change can be challenging. We propose using complex correlation networks to integrate and understand how trees coordinate water- and carbon-related traits under changing climate conditions. We built a correlation network based on 20 traits measured in the wood of *Hymenaea courbaril* (Leguminosae) trees, a species known for its extreme anisohydric water-use strategy, sampled along a climate gradient in Southeastern Brazil. Intercellular to ambient CO_2 concentrations ratio (c_i/c_a, estimated from tree-ring $\delta^{13}C$) is a central network trait for being coordinated with several hydraulic and carbon allocation traits. Trees of *H. courbaril* coordinate these traits along the climate gradient, favoring high c_i/c_a under warm and dry conditions. A high c_i/c_a is only possible through a consistent water supply provided by wider vessels together with the investment on soluble sugars, at the detriment of starch, likely for hydraulic maintenance. Trees also favor heat resistance by investing in cell-wall xylose, another central network trait, from xyloglucans and xylans, at the expense of mannose from glucomannans. Such trade-offs within, and between, structural and non-structural carbon allocation reflect well-known metabolic pathways in plants. In summary, this systemic approach confirms previously reported patterns on leaf physiology, stem hydraulics and carbon adjustments while bringing to light the previously unreported role of cell-wall composition and its fine adjustments to cope with climate change.

1. Introduction

Tropical forests are central components in the global carbon and hydrological cycle (Zuidema et al., 2013; Brienen et al., 2017; Ellison et al., 2017) for exchanging more CO_2 with the atmosphere than any other type of vegetation (Zuidema, 2015; Corlett, 2016) and transpiring more than twice the amount of water vapor in the atmosphere annually (Hetherington and Woodward, 2003). This role of tropical forests on the global carbon and water cycles is mediated by trees' physiology, as they uptake atmospheric CO_2 through stomata at the expense of water losses

* Corresponding author at: Department of Botany, Institute of Biosciences, University of São Paulo, 05508-090 São Paulo, Brazil.
E-mail address: locosselli@yahoo.com.br (G.M. Locosselli).
[1] Authors equally contributed to the paper.

https://doi.org/10.1016/j.ecolind.2021.107798
Received 3 September 2020; Received in revised form 5 April 2021; Accepted 7 May 2021
Available online 21 May 2021

(Tyree and Sperry, 1989; Tyree and Ewers, 1991). The fine tuning of photosynthesis and stomatal conductance in response to environmental changes must be coordinated with adjustments in internal carbon allocation and hydraulic architecture of trees (Van Der Sleen et al., 2015; Brienen et al., 2017; Arco Molina et al., 2018). Long-term adjustments are usually assessed through well-established and newly emerging wood traits (Chave et al., 2006; Poorter et al., 2010; Powell et al., 2017; De Micco et al., 2019; Macieira et al., 2020) that represents physiological and metabolic mechanisms of the above- and below-ground organs responsible for trees' carbon and water fluxes (Beeckman, 2016; Locosselli and Buckeridge, 2017).

Internal carbon allocation in trees depends largely on stomatal conductance and assimilation rates. Both processes are responsible for the control of the intercellular to ambient CO_2 concentrations ratio that is usually estimated through the carbon isotopes signature of the wood of mature trees (McCarroll and Loader, 2004; Lavergne et al., 2020). Once assimilated, carbon undergoes different fates in plants through distinct metabolic pathways. Specific pathways lead to the formation of structural carbohydrates used to synthetize cell-walls. Such structural carbon pools are often assessed by measuring radial growth and / or wood density of trees (Sakschewski et al., 2016; Locosselli and Buckeridge, 2017; Powell et al., 2017; Zuidema et al., 2018), but these approaches fail to give a comprehensive understanding of the fine-tuning of structural carbon pools (Le Gall et al., 2015). Trees may coordinate different carbon pathways for the synthesis of different cell-wall neutral monosaccharides (Fig. 1, Scheller and Ulvskov, 2010; Cosgrove, 2016) that are the building blocks of cell-wall's mechanical stability (Carpita and Gibeaut, 1993; Buckeridge et al., 2008), plasticity (Cosgrove, 2000; Toledano-Thompson et al., 2005) and porosity (Hayashi, 1989; Carpita and Gibeaut, 1993; Cosgrove, 2005; Zykwinska et al., 2005). Carbon may undergo alternative pathways (Fig. 1, Verbančič et al., 2018; Pagliuso et al., 2018) for the synthesis of either short-term reserves in the form of soluble sugars or long-term reserves in the form of starch (Hoch, 2015; Hartmann and Trumbore, 2016; Hartmann et al., 2018). Trees then balance these pathways for structural and non-structural carbon allocation according to their growth strategies and their need to cope with environmental changes (Locosselli and Buckeridge, 2017; Hartmann et al., 2018; Macieira et al., 2020).

A net positive carbon gain presupposes that water is uptaken from the soil, transported in the xylem vessels and transpired through stomata (Tyree and Ewers, 1991, Hoch, 2015; Beeckman, 2016; Hartmann and Trumbore, 2016). Since water is transported against gravity and under tension in the xylem, trees manage the risk of embolism, or hydraulic failure, by co-regulating stomatal conductance and xylem anatomical plasticity (e.g., Tyree and Sperry, 1989; Locosselli and Ceccantini, 2012). Wider vessel elements in lower density can promote carbon gain at the expense of hydraulic safety (Choat et al., 2008; Poorter et al., 2010; Li et al., 2016; Powell et al., 2017), or alternatively trees may invest in safer hydraulics, with narrower vessels at higher density, at the expense of growth. These adjustments in hydraulic traits have been demonstrated before (e.g., Baas et al., 2004; Amaral and Ceccantini, 2011; Jono et al., 2013), but few attempts have been made to integrate water- and carbon-related traits responsible for trees growth and survival under climate change (e.g. Pappas et al. 2016).

Such multi-trait analyses may fail to provide a holistic understanding of plant's mechanisms in response to ongoing climate change partially because of limitations related to frequently used statistical methods, such as Principal Component Analyses (Albert et al., 2010; Lourenço et al., 2020; Macieira et al., 2020) and Path Diagrams (Chapman and McEwan, 2018; Kotowska et al., 2021). Alternative computational methods are now being employed in plant sciences (e.g., Gholami et al., 2017; Kaab et al., 2019; Zhou et al., 2019) and the complex correlation-network is an approach not yet fully explored in the field of plant ecology (He et al., 2020). This approach considers systems not only as a sum of parts but as an accumulation of interconnected subsystems (Barabási and Oltvai, 2004; Koskinen, 2013), such as tree's carbon pools and hydraulics. Graphs are used to represent the networks' topology that consists of a series of nodes, plant traits in this case, and links representing their linear associations (Barabási and Oltvai, 2004; Yamada and Bork, 2009; Cohen and Havlin, 2010). The network properties can be characterized according to the number of links held by each node, the degree centrality, and also by the relative position of a node in the communication of different modules, or subnetworks, the betweenness centrality (Cohen and Havlin, 2010; Toubiana et al., 2013; Jardim et al., 2019). Nodes that combine high values of different centralities may turn out to be more integrative traits that represent most of the network variability. Such structural properties of the networks allow an adequate understanding of multi-trait datasets and further drawing systemic conclusions from their behavior (Yamada and Bork, 2009; Toubiana et al., 2013; Palacios et al., 2019).

To better understand trees' complex responses to ongoing climate change, we studied trees of *Hymenaea courbaril* L., a widely distributed species in the Neotropical lowland forests (Lee and Langenheim, 1975) known for its extreme anisohydric water-use strategy (Werden et al., 2017) characterized by a high stomatal conductance even in the most demanding conditions. This species produces distinct annual tree rings (Luchi, 1998; Westbrook et al., 2006; Lisi et al., 2008) with proven potential to understand environmental variability on trees development, plasticity and growth (e.g., Locosselli et al., 2013; 2016;; Souza et al., 2018; Tiwari et al., 2020). Despite its potential, this target species has not been evaluated before in terms of multi-traits' performance under changing climate conditions. In this study, we analyzed four populations of *H. courbaril* along a climate gradient in Southeastern Brazil that reflects the fundamental expectations of warming and higher precipitation seasonality in the tropics (IPCC, 2014; 2018). Based on the mechanisms described above, we tested the following hypotheses: *I*) the ratio

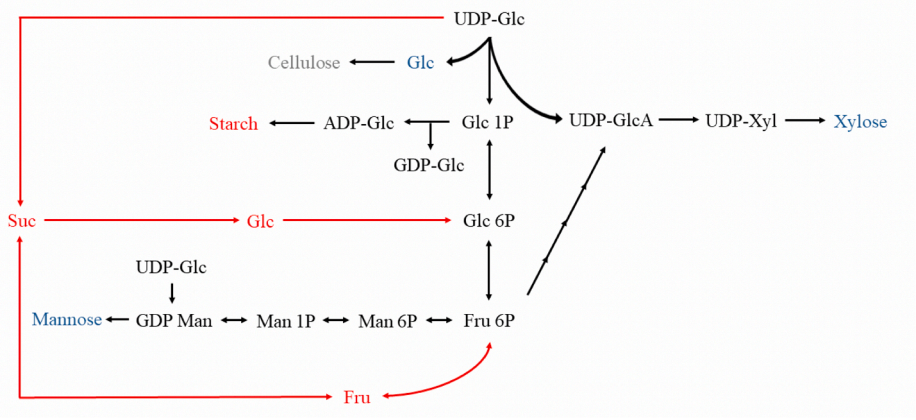

Fig. 1. Simplified carbon metabolic pathways of cell-wall monosaccharides and non-structural carbohydrates synthesis. Glc = Glucose, Fru = Fructose, Suc = Sucrose, GlcA = Glucuronic acid, Xyl = Xylose and Man = Mannose. Black = Precursors of sugars; Red = Non-structural carbohydrates; Blue = Cell-wall monosaccharides. Modified from Verbančič et al. (2017) and Pagliuso et al. (2018). (For interpretation of the references to colour in this figure legend, the reader is referred to the web version of this article.)

between CO_2 concentration in the leaf's mesophyll and in the atmosphere (c_i/c_a) has a central role in the carbon and water balance and, therefore, presents a high degree centrality in the network; *II*) given the different carbon metabolic pathways, trees would display a trade-off between the starch and soluble sugars pools, and a trade-off between non-structural and structural carbon pools; *III*) traits related to the structural carbon pool may also present a high centrality in the network as it consists in the largest carbon sink and it has a central role on trees' growth and survival; *IV*) trees of *H. courbaril* coordinate c_i/c_a and carbon allocation with vessel features to guarantee the water flux necessary for a positive net carbon gain; *V*) *H. courbaril* trees coordinate the main traits, or those with the highest centrality values, to cope with the environmental conditions along a climate gradient.

2. Material and methods

2.1. Species and sampling sites

Hymenaea courbaril L. is usually found in moist broadleaved forests from Northern Mexico to Southeastern Brazil. It belongs to the Leguminosae family, one of the most representative families in the tropical vegetation (Lee and Langenheim, 1975). Trees of *Hymenaea courbaril* reach more than 25 m in height and up to 1.5 m of diameter at breast height (DBH), and are considered emergent trees for growing above the forest canopy. The stem is cylindrical with the rare presence of buttresses. It is a brevi-deciduous species for changing leaves shortly during the dry season (Crankshaw and Langenheim, 1981; Kuhn et al., 2004).

We sampled trees in four Protected Areas from the Atlantic Rain Forest domain along a gradient of climate conditions (Fig. 2, Table S1). Temperature, precipitation, vapor pressure deficit (VPD) and wind speed vary along the gradient towards more demanding atmospheric conditions in the inland. This variability in the climate conditions favors the interactions among different traits supporting the development of the correlation networks (Table S1, Fig. 2). Populations from the four sites are probably from the same phylogeographic group (Ramos et al., 2008), and therefore trait variations are expected to be mostly dependent on environmental conditions.

We sampled 65 trees in these four areas, from two to four increment cores per tree, using a low friction increment borer coupled with a motor drill (Krottenthaler et al., 2015). We carefully chose healthy and emergent trees with no visible signs of injury, decay, or senescence. Out of the sampled trees, we selected four trees from Carlos Botelho State Park, and five trees from the other three sites, based on age above 80 years old, and DBH higher than 55 cm, to avoid ontogenetic biases and the effect of light competition on leaf physiology in the understory (Brienen et al., 2017).

2.2. Studied variables

2.2.1. Tree-ring measurements

All samples were left to dry for a couple of weeks. Samples were polished using sandpapers with grits from 50 to 2,000. All samples were cleaned with pressurized water to remove wood dust from vessel lumen. Tree rings were identified using a stereomicroscope and measured using the Lintab™ 6 system (Rinntech, Heidelberg, Germany). Since we missed the pith in some sampled increment cores, we estimated the number of missing rings to the pith using a modified method from Hietz (2011). False and wedging rings were identified, and tree-ring series synchronized using TSAP-Win™ software (Rinntech, Heidelberg, Germany). Trees from Vassununga State Park and Morro do Diabo State Park, were correctly dated using standard dendrochronological methods (Locosselli et al., 2019). For the other two populations, we crossdated the tree rings among the radii from the same trees. With the tree-ring measurements, we calculated tree's age and basal area increment (BAI, Fig. 3). Because growth may present both short- and long-term trends due to various factors, we calculated mean basal area increment for the last 10, 20, 30, 40, and 50 years (Fig. S1) and we chose the one with the highest correlation values with all other measured traits. We also calculated the number of tree rings in the sapwood (SWr, Fig. 3) and the proportion of sapwood area per total cross-section area (% SWA, Fig. 3).

2.2.2. Wood density

For wood specific gravity analysis, sapwood and heartwood were visually identified and sampled in each specimen (Fig. 3). Samples including multiple tree rings had their wood density measured by the water displacement method (Williamson et al., 2012). All samples were oven-dried at 105 °C for 48 h and reweighed to calculate the initial water content, to estimate the basic specific wood gravity – dry mass/green volume (Chave et al., 2006; see more details in Supplementary Material).

2.2.3. Cell-wall monosaccharides

We used the same samples of sapwood density for cell-wall analyses (Fig. 3). Wood samples were dried at 60 °C to constant weight, and then they were ground in a ball mill (Model TE-350, TECNAL, São Paulo, Brazil). We used 500 mg of the wood sample in four successive extractions with 25 mL of 80% (v/v) ethanol at 80 °C for 20 min and discarded the supernatants to remove the soluble sugars and other soluble compounds. The alcohol-insoluble residue of these extractions was then

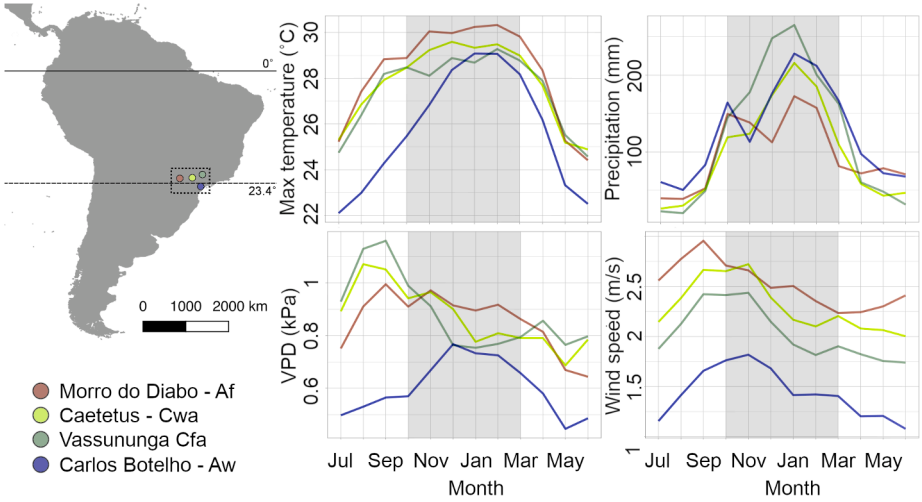

Fig. 2. Sampled populations of *Hymenaea courbaril* (circles) in Southeastern Brazil and respective monthly variation of maximum temperature, precipitation, vapor pressure deficit (VPD) and wind speed. Shaded areas indicate the rainy season. Climate according to Köppen's classification is also provided for each site (Af: tropical with dry season, Cfa: humid subtropical with hot summer, Cwa: humid subtropical with temperate summer, Aw: tropical without dry season). Climate data from Abatzoglou et al. (2018).

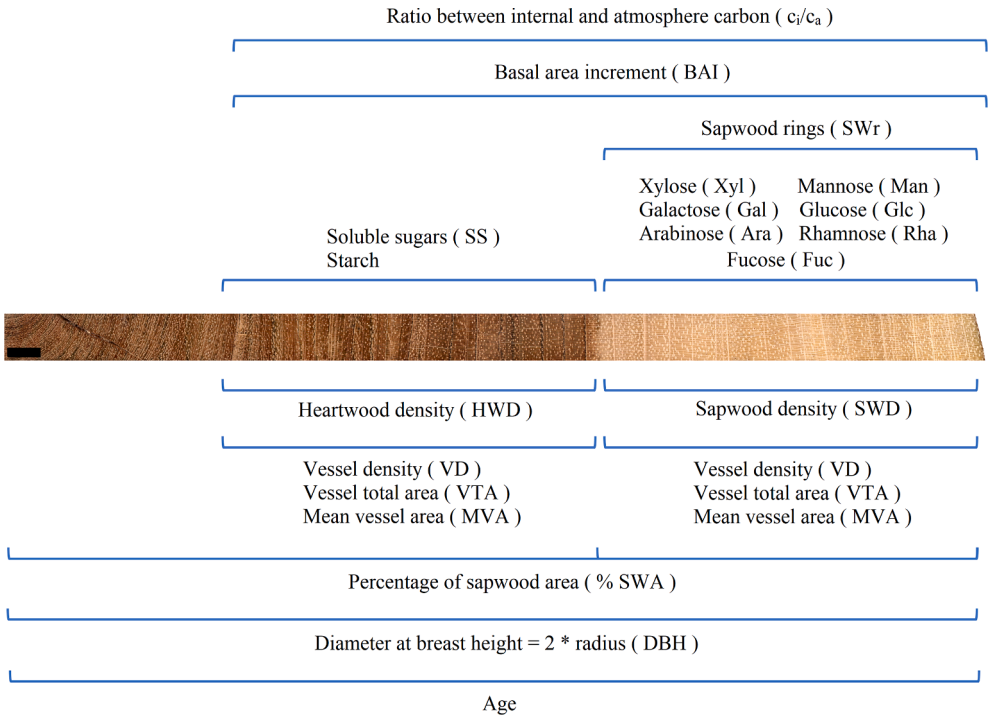

Fig. 3. Traits measured in the wood of four populations of *Hymenaea courbaril* from Southeastern Brazil. Scale bar = 10 mm.

washed with distilled water and dried at 60 °C for 24 h. The cell walls were subjected to successive extractions to solubilize polysaccharide fractions (De Souza et al., 2013; see more details in Supplementary Material), and the fraction yields were obtained gravimetrically.

The monosaccharide composition of the cell wall was obtained by hydrolysis of the alcohol-insoluble residue with 2 M trifluoroacetic acid (TFA) (Saeman et al., 1945; see more details in Supplementary Material). An aliquot of 500 µL of the hydrolysate was analyzed for different monosaccharides by High-Performance Anion Exchange Chromatography with Pulsed Amperometric Detection (HPAEC–PAD) in a Dionex® system (ICS 5000, USA, New Jersey, Manasquan) using a CarboPac PA1 column. The separation was done during a 60 min run with Milli-Q ultrapure water, using a pulse in the first two minutes of 20 mM NaOH at a flow of 1 mL/min. Post-column was used with 500 mM NaOH and flow of 0.5 mL/min. We obtained the concentrations of seven monosaccharides (xylose, galactose, arabinose, mannose, glucose, rhamnose, and fucose) representing the neutral portion of hemicelluloses and pectins of the wood cell-walls.

2.2.4. Non-structural carbohydrates

We used only the heartwood to obtain the concentrations of soluble sugars and starch to avoid the bias of seasonal variation in non-structural carbohydrates (NSC) concentrations in the wood (Fig. 3, Locosselli and Buckeridge 2017). Soluble sugars and starch found in the heartwood are considered 'sequestered' and may represent a record of NSC's concentrations in the wood (Locosselli and Buckeridge, 2017). Total soluble sugar concentrations (SS) were determined by the phenol–sulfuric acid method (Dubois et al., 1956). The determination of starch followed the method by Amaral et al. (2007) and Arenque et al. (2014) through enzymatic extraction (see more details in Supplementary Material).

2.2.5. Ratio of intercellular to ambient CO_2 concentrations

We analyzed the tree-ring carbon isotopes of the last fifty years for each sampled tree. For one tree from Carlos Botelho, data is only available for the last 30 years for technical issues during sample analysis. We used a diamond circular saw (Buehler IsoMet 5000) to produce thin sections of the increment cores. These thin sections were divided into 6 cm segments and placed in Teflon sheets for cellulose extraction using the method by Kagawa et al. (2015) and Schollaen et al. (2017). The ratio values between concentrations of CO_2 in the mesophyll and atmosphere (c_i/c_a, Fig. 3) were estimated using the equation (Farquhar et al., 1982):

$$c_i/c_a = (\delta^{13}C_{plant} - \delta^{13}C_{air} + a) / (b - a)$$

where, a represents the fractionation during diffusion of CO_2 through stomata (–4.4‰), and b represents the fractionation due to carboxylation (–27‰) (Farquhar et al., 1982). Due to the absence of locally measured CO_2, the c_a values were taken from Le Quéré et al. (2018). Because the stable isotopes are subject to short- and long-term trends due to various factors, we calculated mean c_i/c_a for the last 10, 20, 30, 40, and 50 years (Fig. S1) and we chose the one with the highest correlation values with all other traits. (Fig. S1; see more details in Supplementary Material).

2.2.6. Vessel features

Vessels were measured in two groups of ten tree rings representing the decades of the 1950′s and 2000′s to account for vessel tapering in the sampled trees during the analyzed period for BAI and c_i/c_a (Fig. 3). Vessel lumens were highlighted on GIMP software (version 2.10.8, GNU General Public License) to enhance the contrast for the automated detection on ROXAS (version 1.2.0.68, G. von Arx, Birmensdorf, Switzerland). About 10,000 vessels were measured to calculate mean vessel area (MVA), total vessel area (VTA), and vessel density (VD).

2.3. Statistical analyses

We analyzed a total of 20 traits in trees of *H. courbaril* (Table 1, Fig. 3). First, we evaluated the distribution of the values of each trait using histograms (Fig. S2). Then, we calculated the Pearson's correlation (Pearson, 1920) matrix to assess the linear association among the measured continuous variables (Fig. S1) and used this matrix to build complex networks and understand how trees coordinate the measured traits.

Table 1
Minimum, maximum, mean, standard deviation, and respective degree and betweenness centralities of the traits measured in *Hymenaea courbaril* trees from Southeastern Brazil.

Variables	Range	Mean	Std	Centrality values	
				Degree	Betweenness
Age (years)	83 – 273	166	± 60.2	1.54	04
DBH (cm)	55 – 93	75	± 12.8	1.39	18
c_i/c_a	0.58 – 0.68	0.63	± 0.03	3.26	48
SWr	22 – 67	38	± 12.3	3.54	12
% SWA	23 – 54	38	± 8.1	0.81	00
VD (vessels/mm^2)	1.4 – 3.9	2.8	± 0.7	1.71	01
VTA (mm^2)	0.3 – 1.9	1.1	± 0.5	2.70	05
MVA (μm^2 × 10^3)	14 – 39	24	± 0.6	1.57	23
BAI (cm^2/year)	14 – 61	32	± 13.9	3.01	39
SWD (kg/m^3)	0.75 – 1.02	0.87	± 0.07	1.39	00
HWD (kg/m^3)	0.85 – 1.08	0.94	± 0.06	1.29	00
SS (mg/g DM)	1.1 – 3.2	1.9	± 0.6	1.65	04
Starch (mg/g DM)	1.3 – 2.3	1.7	± 0.3	2.02	14
Xyl (mg/g DM)	15.5 – 38.7	31.7	± 5.6	3.29	41
Gal (mg/g DM)	1.6 – 3.2	2.3	± 0.4	1.96	34
Ara (mg/g DM)	1.3 – 4.4	2.3	± 0.8	1.36	48
Man (mg/g DM)	0.9 – 4.4	2.5	± 1.1	1.08	04
Glu (mg/g DM)	3.2 – 6.8	4.9	± 1.1	2.84	68
Rha (mg/g DM)	0.8 – 1.5	1.1	± 0.2	1.39	00
Fuc (mg/g DM)	0.23 – 0.39	0.31	± 0.04	1.11	00

In the complex networks, the measured traits are depicted as nodes, while edges (links) indicate pairwise correlations between component levels. All edges are equally weighed, and represent Pearson's correlation coefficient between component pairs for $\alpha = 0.05$. The importance of the variables in the network structure were estimated based on the centrality analysis. The degree centrality of a given node is proportional to the total number of edges it establishes with other nodes (Barabási and Oltvai, 2004), while the betweenness centrality is a measure of the importance of a node in the connectivity (communication) of different clusters in the network (Freeman, 1978). Networks were built using the BioNetStat package (Jardim et al., 2019; R-Core Team, 2018) that allows a fast and convenient construction of the adjacency matrix from the data table.

Traits were then compared among the study sites. The values of these traits were plotted as boxplots for each sampling site and then compared using Kruskal-Wallis and Dunn tests, for not meeting the criteria of normality and homoscedasticity. The results for the traits representing the main centralities are displayed here, while the results for all other traits are shown in the Supplementary Material.

3. Results

The 20 measured traits showed substantial variation among the sampled trees within our sampling design (Table 1, Fig. S2). The association among the studied traits consisted in a favorable condition to build the final correlation network (Table 1, Fig. 4) that exhibited 33 edges or links that are statistically significant ($\alpha = 0.05$). The main network comprises: c_i/c_a, xylose, mannose, age, mean vessel area, glucose, basal area increment, total vessel area, vessel density, sapwood rings, starch, and soluble sugars. The network also has three additional modules, or sub-networks, one formed by cell-wall monosaccharides (arabinose, galactose, fucose, and rhamnose) that mainly comprise pectins in the wood (0.37% of *Hymenaea courbaril* wood cell wall, Table 2), another comprising wood densities (sapwood and heartwood), and a third comprising percentage of sapwood area and DBH.

The variable c_i/c_a is one of the main degree centralities in the network (Table 1, Fig. 4), indicating that it is correlated to a large number of traits in the studied system. This variable shows positive correlations with sapwood and heartwood densities and cell-wall xylose, but negatively correlated with mannose. In turn, xylose is negatively associated with the concentrations of starch in the heartwood, while mannose is negatively associated with the soluble sugars in the heartwood. These monosaccharides mainly represent hemicelluloses, comprising 38.99% of the dry weight of the wood of *H. courbaril* (Table 2). Soluble sugars and starch also show a negative association between themselves. In addition, c_i/c_a is also positively associated with the mean vessel area, but it shows no correlations with vessel density and vessel total area.

Xylose is also a high degree centrality, and it is positively associated with basal area increment, but negatively associated with age and cell-wall glucose. The number of tree rings in the sapwood is also a high degree and betweenness centralities (Table 1, Fig. 4) in the network, and

Table 2
Cell-wall fractions of *Hymenaea courbaril* trees from Southeastern Brazil.

	Pectins	Lignin	Hemicelluloses	Cellulose
Cell-wall composition (%)	0.37	22.54	38.99	38.09

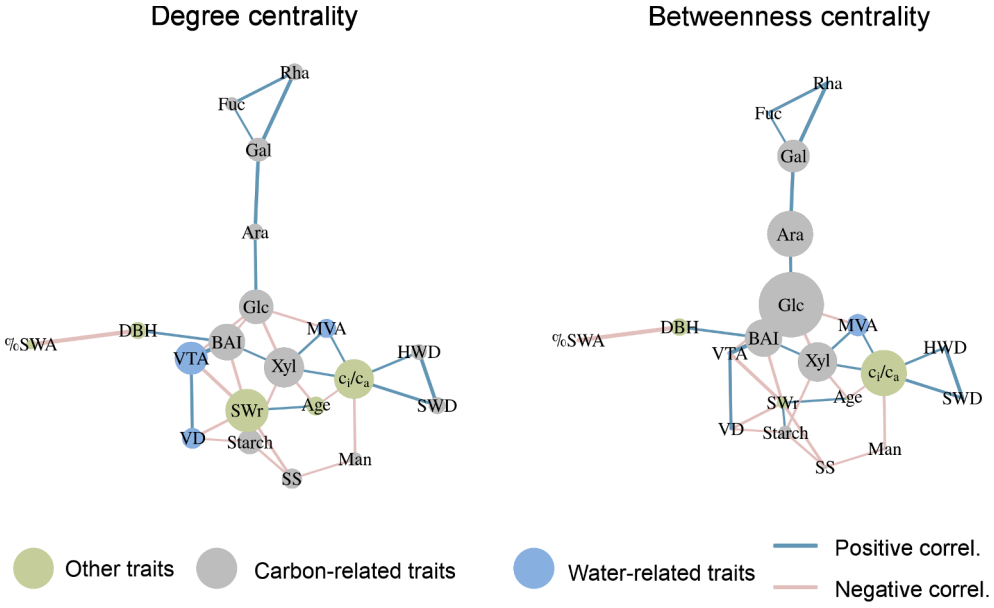

Fig. 4. Complex correlation networks built with 20 traits measured in the wood of *Hymenaea courbaril* trees from Southeastern Brazil. Node sizes are proportional to the values of respective trait centralities (refer to Table 1 for centrality values). The links only show statistically significant correlations between traits ($\alpha = 0.05$), and the colors of the links indicate if correlations are positive (blue), or negative (red). (For interpretation of the references to colour in this figure legend, the reader is referred to the web version of this article.)

it is negatively associated with basal area increment, total vessel area, and vessel density variables, but positively associated with age and starch. Cell-wall glucose and c_i/c_a stand out as the main betweenness centralities in the network (Table 1, Fig. 4). Glucose is the variable with the highest betweenness centrality for connecting the cluster of cell-wall monosaccharides with the main network. The variable c_i/c_a also stands out for having a high value of betweenness centrality for connecting tree density (sapwood and heartwood) with the main network.

Varying environmental conditions lead to significantly different carbon allocation strategies and hydraulic architecture along the studied climate gradient (Fig. 5). Further statistical analysis (using Kruskal-Wallis and Dunn tests) was performed for the comparison of the main centralities' traits among sampling sites. Thus, the network analysis results were extended in a comparative framework reflecting the continental gradient and likely anticipated future climate conditions. Statistically significant differences were particularly pronounced between the two contrasting locations, namely Carlos Botelho and Morro do Diabo State Parks. Higher water availability and lower temperature regimes from Carlos Botelho S.P. are reflected by the lowest values of c_i/c_a ratios, mean vessel area, xylose, and heartwood-soluble sugars (Fig. 5). In contrast, mannose and heartwood-starch concentrations are the highest. In contrast, under the climate conditions of Morro do Diabo S. P., the c_i/c_a ratios, the mean vessel area, and the concentrations of xylose and heartwood-soluble sugars are the highest. On the other hand, mannose and heartwood-starch concentration are the lowest. For all other variables, differences among sites are less evident and often non-significant (Fig. S3).

4. Discussion

4.1. Association among carbon- and water-related traits in the network

We investigated how trees coordinate leaf-level physiology with carbon allocation and stem hydraulics using complex correlation networks. Degree centrality values show that the ratio between the concentrations of CO_2 in the mesophyll and the atmosphere (c_i/c_a) is one of the most integrative traits in the studied system. This central role in the network indicates that trees coordinate leaf-level physiology, namely assimilation and stomatal conductance, with several carbon and hydraulic traits in the wood of *Hymenaea courbaril*.

Leaf-level physiology represented by c_i/c_a is positively associated with xylose content in the cell-walls, another high degree centrality trait, and negatively associated with mannose. Both monosaccharides are part of different hemicellulose classes (xylans and mannans (Hoch, 2007; Schädel et al., 2010a; 2010b) that together represents 39% of the cell wall of *H. courbaril*. Xylans are mostly related to secondary walls, and xyloglucans are mostly related to primary walls of hardwood species, while glucomannans is common to both primary and secondary walls (Buckeridge et al., 2008; Scheller and Ulvskov, 2010). All other cell-wall neutral monosaccharides (galactose, arabinose and rhamnose) form a specific sub-network related to pectins that comprise only 0.37% of *H. courbaril* cell-walls. This sub-network connects to the main network through cell-wall glucose, the highest betweenness centrality in the network, which is a common subunit to cell-wall pectins and hemicelluloses. The observed contrasting association between c_i/c_a, and hemicellulose monosaccharides reflects the metabolic pathways of carbon, in which mannose is produced directly from the uridine diphosphate (UDP) glucose pathway, while xylose is produced via the UDP-Glucuronic acid pathway (Fig. 1).

This association with the carbon metabolic pathways is also evident when evaluating the dynamics of the non-structural carbon reserves. In the present study, we evaluated the concentration of total soluble sugars and starch in the heartwood of trees as a record of their surplus in the sapwood (Würth et al., 2005; Hoch, 2007; Locosselli and Buckeridge, 2017). The concentrations of soluble sugars and starch are negatively associated with mannose and xylose, respectively, showing a trade-off between the deposition of specific structural and non-structural carbohydrates in the wood (Figs. 1 and 4). These trade-offs reflect again the contrasting pathways of carbohydrate metabolism in plants. Whereas the UDP-Glucose (Glc) pyrophosphorylase (UGPase) pathway leads to the allocation of structural carbohydrates and soluble sugars during plant development and growth, the adenosine diphosphate (ADP)-Glc pyrophosphorylase (AGPase) pathway results in the formation of starch as carbon reserves (Horacio and Martinez-Noel, 2013; Janse van Rensburg and Van den Ende, 2018; Pagliuso et al., 2018).

It is also expected that trees coordinate both c_i/c_a and carbon

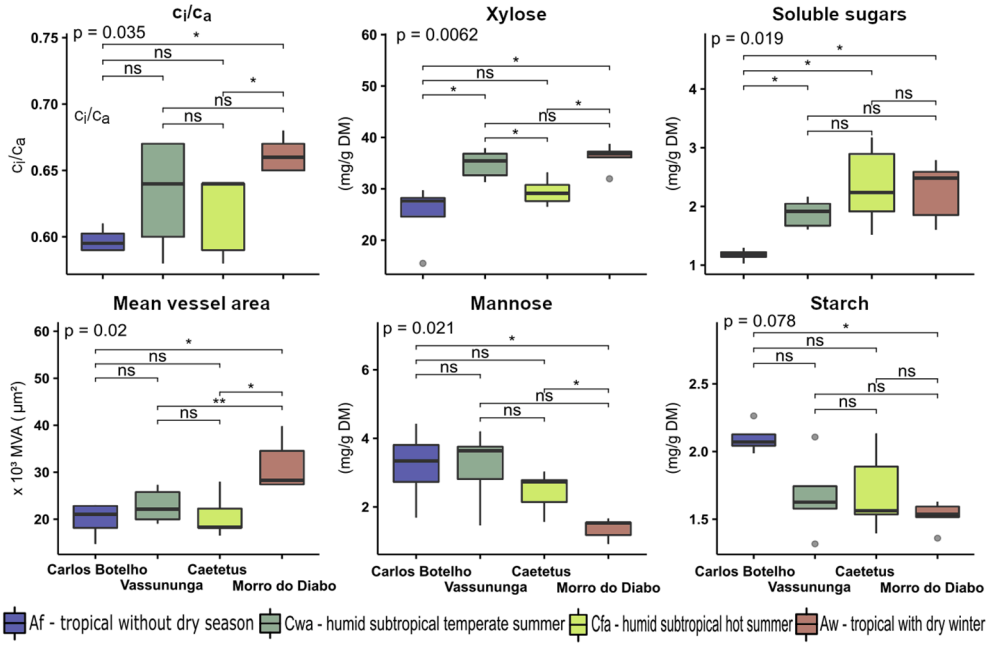

Fig. 5. Comparison of the variables comprising key centralities in the complex networks, namely: intercellular to ambient CO_2 concentrations ratio (c_i/c_a), cell-wall xyloses in the sapwood (SW Xyl), soluble sugars in the heartwood (HW Sugars), mean vessel area (MVA), cell-wall mannoses in the sapwood (SW Man), and starch in the heartwood (HW starch), among four different cities across a climate gradient. * significant for $\alpha = 0.05$, ns for non-significant.

allocation with tree's hydraulic traits (Choat et al., 2008; Powell et al., 2017). Wider vessels are positively associated with high c_i/c_a for an efficient water transport (Poorter et al., 2010; Zanne et al., 2010) together with the investment in cell-wall xylose at the expense of cell-wall glucose and pectin-related monosaccharides. Vessel total area, on the other hand, is not associated with c_i/c_a, but it strongly contributes to the basal area increment of trees for the high volumetric expansion of vessels during wood development (Poorter et al., 2010; Beeckman, 2016; Tng et al., 2018). Although wood hydraulic traits are at the network periphery, these associations further confirm the coordination of leaf physiology not only with carbon allocation but also with the water transport in trees.

Other traits commonly used in the literature like the percentage of sapwood area and DBH form a second sub-network. This is an intriguing result because the percentage of sapwood area is a critical trait in functional ecology (e.g., Westoby and Wright, 2006; Sterck et al., 2011; Beyer et al., 2018). This is also true for wood density, a highly regarded wood trait (Chave et al., 2006), that forms a third subnetwork. The poor connection of these two sub-networks to the main network points to possible limitations of the choice of traits in the present study and might be explained by other developmental mechanisms within the stem that have not been considered here. Alternatively, the number of tree rings in the sapwood stands out as the highest degree centrality in the network. This highly integrative trait points to a more conservative strategy as trees grow older, like the reduction in hydraulic conductivity and growth, and a higher investment in long-term reserves in old living parenchyma cells (Richardson et al., 2013; 2015;; Beeckman, 2016; Hartmann and Trumbore, 2016; Tng et al., 2018).

4.2. Coordination of traits along a climate gradient

A significant share of the network's variability reflects the coordination of the measured traits in the trees along a gradient of temperature and water availability. Trees of *H. courbaril* showed increased c_i/c_a along drying conditions, which seems in contradiction with the expected reduction of stomatal conductance (g_s) under more evaporative demands (Tan et al., 2017; Dewar et al., 2018). Water deficit, however, may have no direct effect on g_s according to species growth strategies up to certain thresholds (Lawlor and Tezara, 2009; Peri et al., 2009; Ashraf and Harris, 2013), and *H. courbaril* does have proven higher thermal tolerance of the leaves than other tropical tree species (Tiwari et al., 2020), sustaining high xylem and stomatal conductance at consistently low leaf water potentials (Brodribb et al., 2003; Klein, 2014). For these strategies, *H. courbaril* is considered a drought tolerant species that adopts an extreme anisohydric water-use strategy (Werden et al., 2017). To keep pace with the increasing c_i/c_a, trees of *H. courbaril* rely on wider vessels to guarantee sustained water fluxes (Poorter et al., 2010; Zanne et al., 2010, Fig. 6), but at the risk of frequent hydraulic failures.

Sugar-mediated repair mechanisms are likely needed to guarantee a constant water flux in the more seasonal and warmer site. Under these conditions, soluble sugars are known to be used for embolism reversal by creating osmotic gradient (Brodersen et al., 2010), and contributing to the synthesis of surfactants for nanotubules stabilization in the pit membranes (De Baedemaeker et al., 2017). This increased investment on soluble sugar was observed before in seedlings of different tree species under water stress, including seedlings of *H. courbaril* (Zhang et al., 2015; Souza et al., 2018) and mature trees of this species in the present study. The studied trees also showed higher xylose in the wood, likely from xyloglucan a key polysaccharide in the wood (Hayashi and Kaida, 2011; Seale, 2020), that is known to strengthen the connections between primary and secondary cell walls and increase the tolerance to heat stress (Le Gall et al., 2015). In the other extreme of the climate gradient, we observed that trees invest in cell-wall mannose, and on starch as a non-structural carbohydrate reserve. Such long-term reserves represent a more conservative strategy that may guarantee growth and survival of trees in the long run (Hartmann and Trumbore, 2016; Locosselli and Buckeridge, 2017). This high investment in long-term reserves together with lower metabolic rates and are indeed related to longer-lifespans (López et al., 2009; Camarero et al., 2015; Hartmann and Trumbore, 2016; Brienen et al., 2020), that tends to increase towards the wet tropics (Locosselli et al., 2020) as observed in the present study (Fig. S3). Altogether, these results consist in a strong evidence that trees modulate hydraulic architecture, non-structural carbohydrates reserves and cell-wall composition to couple with changing environmental conditions, which opens new avenues for studies of tree' ecophysiology, particularly in the context of future climate change.

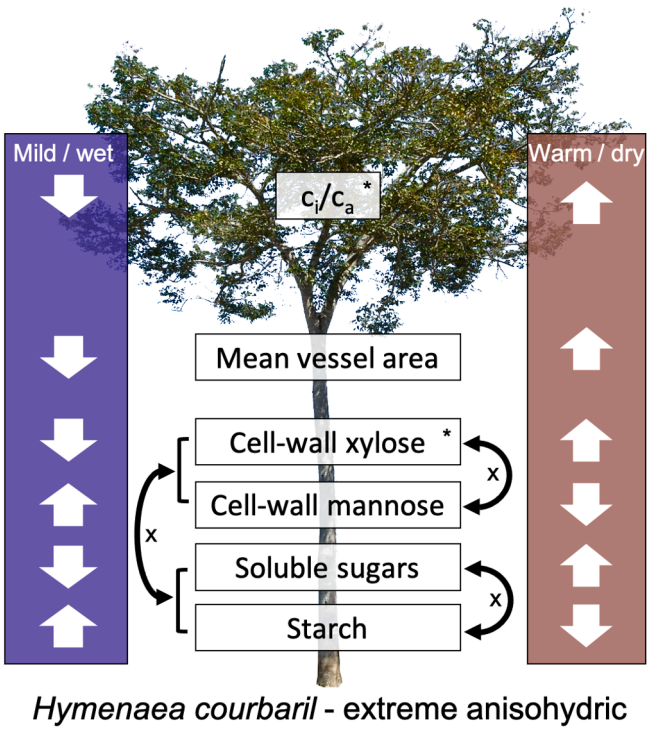

Fig. 6. Summary of the coordination among leaf-level physiology, stem hydraulics and carbon pools in trees of *Hymenaea courbaril* along a climate gradient in Southeastern Brazil. The white arrows indicate if the values increase or decrease under different climate conditions, the black arrows indicate trade-offs, and * indicates high degree centrality in the correlation networks.

5. Conclusions

The present study brings novel insights about the balance between carbon- and water-related traits in the wood of tropical trees (Fig. 6) based on complex correlation networks. The results using this systemic approach indicate that trees' strategy to cope with climate change requires a fine-tuning in carbon uptake, carbon allocation pathways, and hydraulic architecture of trees. The expected associations among the measured traits, especially those representing trade-offs, were all clear in the graphs attesting the power of this approach in trait analyses. The centrality values then highlighted the relative role of the measured traits in the network. A significant part of the association among the high centrality traits, including leaf physiology, wood hydraulics, structural and non-structural carbon allocation, depend on the variability of the climate conditions. The observed changes in cell-wall composition, which may occur at the expense of both starch and soluble sugars, consist of a novel pattern not reported before in mature trees inhabiting their natural environment. Although the mechanisms behind the variability in cell-wall composition need to be further clarified in *H. courbaril* and other tree species, cell-wall monosaccharides emerge as valuable and integrative traits to be used in studies concerning trees' responses to climate change.

Declaration of Competing Interest

The authors declare that they have no known competing financial interests or personal relationships that could have appeared to influence the work reported in this paper.

Acknowledgments

Authors thank all local guides for support in the field, and Heiko Baschek, Paula Alécio, Gisele Costa, and Tássia Cristina dos Santos, Eglee Igarashi and Viviane Lopes for laboratory support, and Dr Roel Brienen and Dr Bruno Cintra for valuable discussion, and Ricardo Cardim for the image of *H. courbaril* tree. We also thank Débora Pagliuso for her help with the metabolic pathways. Authors thank São Paulo Research Foundation – FAPESP for financial support (2008/57908-6, 2012/50457-4, 2014/50884-5, 2015/25511-3, 2017/50085-3, 2019/08783-0, 2020/09251-0), Deutsche Forschungsgemeinschaft (DFG) (AN 214/10-1, AN 214/10-2), Fundação de Amparo à Pesquisa e Inovação do Estado do Espírito Santo – FAPES (2020-FBRW1), and National Council for Scientific and Technological Development (CNPq 574002/2008-1, 465319/2014-9).

Appendix A. Supplementary data

Supplementary data to this article can be found online at https://doi.org/10.1016/j.ecolind.2021.107798.

References

Abatzoglou, J.T., Dobrowski, S.Z., Parks, S.A., Hegewisch, K.C., 2018. TerraClimate, a high-resolution global dataset of monthly climate and climatic water balance from 1958–2015. Scientific Data 5, 170191.

Albert, C.H., Thuiller, W., Yoccoz, N.G., Douzet, R., Aubert, S., Lavorel, S., 2010. A multi-trait approach reveals the structure and the relative importance of intra- *vs* interspecific variability in plant traits. Funct. Ecol. 24 (6), 1192–1201.

Amaral, M.M., Ceccantini, G., 2011. The endoparasite *Pilostyles ulei* (Apodanthaceae – Cucurbitales) influences wood structure in three host species of *Mimosa*. IAWA J. 32 (1), 1–13.

Amaral, L.I.V., Gaspar, M., Costa, P.M.F., Aidar, M.P.M., Buckeridge, M.S., 2007. Novo método enzimático rápido e sensível de extração e dosagem de amido em materiais vegetais. Hoehnea 34 (4), 425–431.

Arco Molina, J.G., Helle, G., Hadad, M.A., Roig, F.A., 2018. Variations in the intrinsic water-use efficiency of north Patagonian forests under a present climate change scenario: Tree age, site conditions and long-term environmental effects. Tree Physiol. 39 (4), 661–678.

Arenque, B.C., Grandis, A., Pocius, O., De Souza, A.P., Buckeridge, M.S., 2014. Responses of *Senna reticulata*, a legume tree from the Amazonian floodplains, to elevated atmospheric CO_2 concentration and waterlogging. Trees Struct. Funct. 28 (4), 1021–1034.

Ashraf, M.H.P.J.C., Harris, P.J., 2013. Photosynthesis under stressful environments: an overview. Photosynthetica 51 (2), 163–190.

Baas, P., Ewers, F.W., Davis, S.D., Wheeler, E., 2004. Evolution of xylem physiology. In: R. Hemsley and I. Poole (eds). The Evolution of Plant Physiology. Academic Press, Chap. 15, 273-295.

De Baedemaeker, N.J.F., Salomón, R.L., De Roo, L., Steppe, K., 2017. Sugars from woody tissue photosynthesis reduce xylem vulnerability to cavitation. New Phytol. 216 (3), 720–727.

Barabási, A.L., Oltvai, Z.N., 2004. Network biology: Understanding the cell's functional organization. Nat. Rev. Genet. 5 (2), 101–113.

Beeckman, H., 2016. Wood anatomy and trait-based ecology. IAWA J. 37 (2), 127–151.

Beyer, F., Jäck, O., Manzoni, S., Weih, M., 2018. Relationship between foliar $\delta^{13}C$ and sapwood area indicates different water use patterns across 236 *Salix* genotypes. Trees 32 (6), 1737–1750.

Brienen, R.J.W., Caldwell, L., Duchesne, L., Voelker, S., Barichivich, J., Baliva, M., Ceccantini, G., Di Filippo, A.D., Helema, S., Locosselli, G.M., Lopez, L., Piovesan, G., Schöngart, J., Villalba, R., Gloor, R., 2020. Forest carbon sink neutralized by pervasive growth-lifespan trade-offs. Nat. Commun. 11, 4241.

Brienen, R.J.W., Gloor, E., Clerici, S., Newton, R., Arppe, L., Boom, A., Bottrell, S., Callaghan, M., Heaton, T., Helama, S., Helle, G., Leng, M.J., Mielikäinen, K., Oinonen, M., Timonen, M., 2017. Tree height strongly affects estimates of water-use efficiency responses to climate and CO_2 using isotopes. Nat. Commun. 8 (1), 288–298.

Brodersen, C.R., McElrone, A.J., Choat, B., Matthews, M.A., Shackel, K.A., 2010. The dynamics of embolism repair in xylem: in vivo visualizations using high-resolution computed tomography. Plant Physiol. 154, 1088–1095.

Brodribb, T.J., Holbrook, N.M., Edwards, E.J., Gutiérrez, M.V., 2003. Relations between stomatal closure, leaf turgor and xylem vulnerability in eight tropical dry forest trees. Plant Cell Environ. 26, 443–450.

Buckeridge, M.S., Cavalari, A.A., Silva, G.B., 2008. Parede Celular. In: Kerbauy, G.B. (ed.) Fisiologia Vegetal. Guanabara Koogan, Rio de Janeiro 2, 165–181.

Camarero, J.J., Gazol, A., Sangüesa-Barreda, G., Oliva, J., Vicente-Serrano, S.M., 2015. To die or not to die: Early warnings of tree dieback in response to severe drought. J. Ecol. 103 (1), 44–57.

Carpita, N.C., Gibeaut, D.M., 1993. Structural models of primary cell walls in flowering plants: Consistency of molecular structure with the physical properties of the walls during growth. Plant J. 3 (1), 1–30.

Chapman, J.I., McEwan, R.W., 2018. The role of environmental filtering in structuring Appalachian tree communities: Topographic influences on functional diversity are mediated through soil characteristics. Forests 9 (1), 19.

Chave, J., Muller-Landau, H.C.M., Baker, T.R., Easdale, T.A., Steege, H., Webb, C.O., 2006. Regional and phylogenetic variation of wood density across 2456 Neotropical tree species. Ecol. Appl. 16 (6), 2356–2367.

Choat, B., Cobb, A.R., Jansen, S., 2008. Structure and function of bordered pits: New discoveries and impacts on whole-plant hydraulic function. New Phytol. 177 (3), 608–626.

Cohen, R., Havlin, S., 2010. Complex networks: structure, robustness and function. Cambridge University Press, The Edinburgh Building, Cambridge.

Corlett, R.T., 2016. The impacts of droughts in tropical forests. Trends Plant Sci. 21 (7), 584–593.

Cosgrove, D.J., 2016. Plant cell wall extensibility: Connecting plant cell growth with cell wall structure, mechanics, and the action of wall-modifying enzymes. J. Exp. Bot. 67 (2), 463–473.

Cosgrove, D.J., 2005. Growth of the plant cell wall. Nat. Rev. 6 (11), 850–861.

Cosgrove, D.J., 2000. Loosening of plant cell walls by expansins. Nature 407, 321–326.

Crankshaw, D.R., Langenheim, J.H., 1981. Variation in terpenes and phenolics through leaf development in *Hymenaea* and its possible significance to herbivory. Biochem. Syst. Ecol. 9 (2/3), 115–124.

De Souza, A.P., Leite, D.C.C., Pattathil, S., Hahn, M.G., Buckeridge, M.S., 2013. Composition and structure of sugarcane cell wall polysaccharides: Implications for second-generation bioethanol production. Bioenergy Res. 6 (2), 564–579.

De Micco, V., Carrer, M., Rathgeber, C.B., Camarero, J.J., Voltas, J., Cherubini, P., Battipaglia, G., 2019. From xylogenesis to tree rings: wood traits to investigate tree response to environmental changes. IAWA J. 40 (2), 155–182.

Dewar, R., Mauranen, A., Mäkelä, A., Hölttä, T., Medlyn, B., Vesala, T., 2018. New insights into the covariation of stomatal, mesophyll and hydraulic conductances from optimization models incorporating nonstomatal limitations to photosynthesis. New Phytol. 217 (2), 571–585.

Dubois, M., Giles, K.A., Hamilton, J.K., Rebers, P.A., Smith, F., 1956. Colorimetric method for determination of sugars and related substances. Anal. Chem. 28 (3), 350–356.

Ellison, D., Morris, C.E., Locatelli, B., Sheil, D., Cohen, J., Murdiyarso, D., Gutierrez, V., et al., 2017. Trees, forests and water: Cool insights for a hot world. Global Environ. Chang. 43, 51–61.

Farquhar, G.D., O'Leary, M.H., Berry, J.A., 1982. On the relationship between carbon isotope discrimination and intercellular carbon dioxide concentration in leaves. Aust. J. Plant Physiol. 9 (2), 121–137.

Freeman, L.C., 1978. Centrality in social networks conceptual clarification. Soc. Netw. 1 (3), 215–239.

Gholami, V., Jolandan, M.A., Torkman, J., 2017. Evaluation of climate change in northern Iran during the last four centuries by using dendroclimatology. Nat. Hazards 85, 1835–1850.

Hartmann, H., Trumbore, S., 2016. Understanding the roles of non-structural carbohydrates in forest trees – from what we can measure to what we want to know. New Phytol. 211 (2), 386–403.

Hartmann, H., Adams, H.D., Hammond, W.M., Hoch, G., Landhäusser, S.M., Wiley, E., Zaehle, S., 2018. Identifying differences in carbohydrate dynamics of seedlings and mature trees to improve carbon allocation in models for trees and forests. Environ. Exper. Bot. 152, 7–18.

Hayashi, T., 1989. Xyloglucans in the primary cell wall. Annu. Rev. Plant Physiol. Plant Mol. Biol. 40 (1), 139–168.

Hayashi, T., Kaida, R., 2011. Functions of xyloglucan in plant cells. Molecular Plant 4 (1), 17–24.

He, N., Li, Y., Liu, C., Xu, L., Li, M., Zhang, J., He, J., Tang, Z., Han, X., Ye, Q., Xiao, C., Yu, Q., Liu, S., Sun, W., Niu, S., Li, S., Sack, L., Yu, G., 2020. Plant trait networks: improved resolution of the dimensionality of adaptation. Trends Ecol. Evol. 35 (10), 908–918.

Hetherington, A.M., Woodward, F.I., 2003. The role of stomata in sensing and driving environmental change. Nature 424 (6951), 901–908.

Hietz, P., 2011. A simple program to measure and analyse tree rings using Excel. R and SigmaScan. Dendrochronologia 29 (4), 245–250.

Hoch, G., 2015. Carbon reserves as indicators for carbon limitation in trees. In: Progress in Botany. Springer, Cham, pp. 321–346.

Hoch, G., 2007. Cell wall hemicelluloses as mobile carbon stores in non-reproductive plant tissues. Funct. Ecol. 21 (5), 823–834.

Horacio, P., Martinez-Noel, G., 2013. Sucrose signaling in plants: a world yet to be explored. Plant Signal. Behav. 8 (3), e23316.

IPCC, 2014. Annex II: Glossary. In: Barros, V.R., Field, C.B., Dokken, D.J., Mastrandrea, M.D., Mach, K.J., Bilir, T.E., et al., IPCC (eds.) Climate Change 2014: Impacts, Adaptation, and Vulnerability. Part B: Regional Aspects. Contribution of Working Group II to the Fifth Assessment Report of the Intergovernmental Panel on Climate Change. Cambridge: Cambridge University Press, 1757–1776.

IPCC, 2018. Summary for Policymakers. In: Allen, M., Babiker, M., Chen, Y., Coninck, H. de, Connors, S., et al., IPCC (eds.) Global Warming of 1.5 °C: An IPCC Special Report on the impacts of global warming of 1.5 °C above pre-industrial levels and related global greenhouse gas emission pathways, in the context of strengthening the global response to the threat of climate change, sustainable development, and efforts to eradicate poverty. Geneva: World Meteorological Organization, 1–32.

Janse van Rensburg, H.C., Van den Ende, W., 2018. UDP-Glucose: A potential signaling molecule in plants? Front. Plant Sci. 8, 2230.

Jardim, V.C., Santos, S.S., Fujita, A., Buckeridge, M.S., 2019. BioNetStat: A tool for biological networks differential analysis. Front. Genet. 10, 594–605.

Jono, V., Locosselli, G.M., Ceccantini, G., 2013. The influence of tree size and microenvironmental changes on the wood anatomy of *Roupala rhombifolia*. IAWA J. 34 (1), 88–106.

Kaab, A., Sharifi, M., Mobli, H., Nabavi-Pelesarei, A., Chau, K., 2019. Combined life cycle assessment and artificial intelligence for prediction of output energy and environmental impacts of sugarcane production. Sci. Total Environ. 664, 1005–1019.

Kagawa, A., Sano, M., Nakatsuka, T., Ikeda, T., Kubo, S., 2015. An optimized method for stable isotope analysis of tree rings by extracting cellulose directly from cross sectional laths. Chem. Geol. 393, 16–25.

Klein, T., 2014. The variability of stomatal sensitivity to leaf water potential across tree species indicates a continuum between isohydric and anisohydric behaviours. Funct. Ecol. 28, 1313–1320.

Koskinen, K.U., 2013. Systemic View and Systems Thinking. In: Knowledge Production in Organizations. Springer, Heidelberg, pp. 13–33.

Kotowska, M.M., Link, R.M., Röll, A., Hertel, D., Hölscher, D., Waite, P.A., Moser, G., Tjoa, A., Leuschner, C., Schuldt, B., 2021. Effects of wood hydraulic properties on water use and productivity of tropical rainforest trees. Front. For. Glob. Change 3, 154.

Krottenthaler, S., Pitsch, P., Helle, G., Locosselli, G.M., Ceccantini, G., Altman, J., Svoboda, M., Dolezal, J., Scheleser, G., Anhuf, D., 2015. A power-driven increment borer for sampling high-density tropical wood. Dendrochronologia 36, 40–44.

Kuhn, U., Rottenberger, S., Biesenthal, T., Wolf, A., Schebeske, G., Ciccioli, P., Kesselmeier, J., 2004. Strong correlation between isoprene emission and gross photosynthetic capacity during leaf phenology of the tropical tree species *Hymenaea courbaril* with fundamental changes in volatile organic compounds emission composition during early leaf development. Plant Cell Environ. 27 (12), 1469–1485.

Lavergne, A., Voelker, S., Csank, A., Graven, H., de Boer, H.J., Daux, V., Robertson, I., Dorado-Liñán, I., Martínez-Sancho, E., Battipaglia, G., Bloomfield, K.J., Still, C.J., Meinzer, F.C., Dawson, T.E., Camarero, J.J., Clisby, R., Fang, Y., Menzel, A., Keen, R. M., Roden, J.S., Prentice, I.C., 2020. Historical changes in the stomatal limitation of photosynthesis: empirical support for an optimality principle. New Phytol. 225 (6), 2484–2497.

Lawlor, D.W., Tezara, W., 2009. Causes of decreased photosynthetic rate and metabolic capacity in water-deficient leaf cells: a critical evaluation of mechanisms and integration of processes. Ann. Bot. 103 (4), 561–579.

Le Gall, H., Philippe, F., Domon, J.M., Gillet, F., Pelloux, J., Rayon, C., 2015. Cell wall metabolism in response to abiotic stress. Plants 4 (1), 112–166.

Le Quéré, C., Andrew, R.M., Friedlingstein, P., Sitch, S., Hauck, J., Pongratz, J., Pickers, P.A., et al., 2018. Global Carbon Budget 2018. Earth Syst. Sci. Data 10 (4), 2141–2194.

Lee, Y.T., Langenheim, J.H., 1975. A systematic revision of the genus *Hymenaea* (Leguminosae; Caesalpinioideae; Detarieae). Univ. Calif. Publ. Bot. 69, 1–109.

Li, S., Lens, F., Espino, S., Karimi, Z., Klepsch, M., Schenk, J., Schmitt, M., Schuldt, B., Jansen, S., 2016. Intervessel pit membrane thickness as a key determinant of embolism resistance in angiosperm xylem. IAWA J. 37 (2), 152–171.

Lisi, C.S., Tomazello, M., Botosso, P.C., Roig, F.A., Maria, V.R.B., Ferreira-Fedele, L., Voigt, A.R.A., 2008. Tree-ring formation, radial increment periodicity and phenology of tree species from a seasonal semi-deciduous forest in southeast Brazil. IAWA J. 29 (2), 189–207.

Locosselli, G.M., Buckeridge, M.S., 2017. Dendrobiochemistry, a missing link to further understand carbon allocation during growth and decline of trees. Trees Struct. Funct. 31 (6), 1745–1752.

Locosselli, G.M., Ceccantini, G., 2012. Plasticity of stomatal distribution pattern and stem tracheid dimensions in *Podocarpus lambertii:* an ecological study. Ann. Bot. 110 (5), 1057–1066.

Locosselli, G.M., Brienen, R.J.W., Leite, M.S., Gloor, M., Krothentaller, S., de Oliveira, A. A., Barichivich, J., Anhuf, D., Ceccantini, G., Schöngart, J., Buckeridge, M., 2020. Global tree-ring analysis reveals rapid decrease in tropical tree longevity with temperature. Proc. Natl. Acad. Sci. 117 (52), 33358–33364.

Locosselli, G.M., Krothentaller, S., Pitsch, P., Anhuf, D., Ceccantini, G., 2019. Impact of temperature on the growth of a Neotropical tree species (*Hymenaea courbaril*, Fabaceae) at its distribution limit. Int. J. Biometereol. 63 (12), 1683–1689.

Locosselli, G.M., Schöngart, J., Ceccantini, G., 2016. Climate/growth relations and teleconnections for a *Hymenaea courbaril* (Leguminosae) population inhabiting the dry forest on karst. Trees 30 (4), 1127–1136.

Locosselli, G.M., Buckeridge, M.S., Moreira, M.Z., Ceccantini, G., 2013. A multi-proxy dendroecological analysis of two tropical species (*Hymenaea* spp., Leguminosae) growing in a vegetation mosaic. Trees 27 (1), 25–36.

López, B.C., Gracia, C.A., Sabatée, S., Keenan, T., 2009. Assessing the resilience of Mediterranean holm oaks to disturbances using selective thinning. Acta Oecol. 35 (6), 849–854.

Lourenço, J., Newman, E.A., Milanez, C.R.D., Thomaz, L.D., Enquist, B.J., 2020. Assessing trait driver theory along abiotic gradients in tropical plant communities. bioRxiv.

Luchi, A.E., 1998. Periodicidade de crescimento em *Hymenaea courbaril* L. e anatomia ecológica do lenho de espécies de mata ciliar. PhD Thesis, Instituto de Biociências, Universidade de São Paulo, São Paulo.

Macieira, B.P.B., Locosselli, G.M., Buckeridge, M.S., Hartmann, H., Cuzzuol, G.R.F., 2020. Stem and leaf functional traits allow successional classification in six pioneer and non-pioneer tree species in the Tropical Moist Broadleaved Forests. Ecol. Indic. 113, 106254.

McCarroll, D., Loader, N.J., 2004. Stable isotopes in tree rings. Quat. Sci. Rev. 23, 771–801.

Pagliuso, D., Grandis, A., Igarashi, E.S., Lam, E., Buckeridge, M.S., 2018. Correlation of apiose levels and growth rates in duckweeds. Front. Chem. 6, 291–300.

Palacios, C.J., Grandis, A., Carvalho, V.J., Salatino, A., Buckeridge, M.S., 2019. Isolated and combined effects of elevated CO_2 and high temperature on the whole-plant biomass and the chemical composition of soybean seeds. Food Chem. 275, 610–617.

Pappas, C., Fatichi, S., Burlando, P., 2016. Modelling terrestrial carbono and water dynamics across climatic gradients: does plant trait diversity matter? New Phytol. 209, 137–151.

Pearson, K., 1920. Notes on the History of Correlation. Biometrika 13 (1), 25–45.

Peri, P.L., Pastur, G.M., Lencinas, M.V., 2009. Photosynthetic response to different light intensities and water status of two main *Nothofagus* species of southern Patagonian forest. Argentina. J. For. Sci. 55 (3), 101–111.

Poorter, L., McDonald, I., Alarcón, A., Fichtler, E., Licona, J., Peña-Claros, M., Sterck, F., Villegas, Z., Sass-Klaasen, U., 2010. The importance of wood traits and hydraulic conductance for the performance and life history strategies of 42 rainforest tree species. New Phytol. 185 (2), 481–492.

Powell, T.L., Wheeler, J.K., de Oliveira, A.A., da Costa, A.C.L., Saleska, S.R., Meir, P., Moorcroft, P.R., 2017. Differences in xylem and leaf hydraulic traits explain differences in drought tolerance among mature Amazon rainforest trees. Glob. Change Biol. 23 (10), 4280–4293.

Ramos, A.C.S., De Lemos-Filho, J.P., Lovato, M.B., 2008. Phylogeographical structure of the Neotropical forest tree *Hymenaea courbaril* (Leguminosae: Caesalpinioideae) and its relationship with the vicariant *Hymenaea stigonocarpa* from Cerrado. J. Hered. 100 (2), 206–216.

Richardson, A.D., Carbone, M.S., Huggett, B.A., Furze, M.E., Czimczik, C.I., Walker, J.C., Xu, X., Schaberg, P.G., Murakami, P., 2015. Distribution and mixing of old and new non-structural carbon in two temperate trees. New Phytol. 206 (2), 590–597.

Richardson, A.D., Carbone, M.S., Keenan, T.F., Czimczik, C.I., Hollinger, D.Y., Murakami, P., Schaberg, P.G., Xu, X., 2013. Seasonal dynamics and age of stemwood non-structural carbohydrates in temperate forest trees. New Phytol. 197 (3), 850–861.

Saeman, J.F., Harris, E.E., Kline, A.A., 1945. Analysis of wood sugar. Ind. Eng. Chem. Res. 17 (2), 95.

Sakschewski, B., Von Bloh, W., Boit, A., Poorter, L., Peña-Claros, M., Heinke, J., Joshi, J., Thonicke, K., 2016. Resilience of Amazon forests emerges from plant trait diversity. Nat. Clim. Change 6 (11), 1032–1036.

Schädel, C., Blöchl, A., Richter, A., Hoch, G., 2010a. Quantification and monosaccharide composition of hemicelluloses from different plant functional types. Plant Physiol. Biochem. 48 (1), 1–8.

Schädel, C., Richter, A., Blöchl, A., Hoch, G., 2010b. Hemicellulose concentration and composition in plant cell walls under extreme carbon source–sink imbalances. Physiol. Plant. 139 (3), 241–255.

Scheller, H.V., Ulvskov, P., 2010. Hemicelluloses. Annu. Rev. Plant Biol. 61, 263–289.

Schollaen, K., Baschek, H., Heirich, I., Slotta, F., Pauly, M., Helle, G., 2017. A guideline for sample preparation in modern tree-ring stable isotope research. Dendrochronologia 44, 133–145.

Seale, M., 2020. Cell Wall Remodeling during Wood Development. Am. Soc. Plant Biol. 1800–1801.

Souza, L.C., Luz, L.M., Martins, J.T.S., Neto, C.F.O., Palheta, J.G., Oliveira, T.B., Alves, E. C., Almeida, R.F., Oliveira, R.L.L., Costa, R.C.L., Vilhena, N.Q., 2018. Osmoregulation in *Hymenaea courbaril* and *Hymenaea stigonocarpa* under water stress and rehydration. J. For. Res. 29 (6), 1475–1479.

Sterck, F., Markesteijn, L., Schieving, F., Poorter, L., 2011. Functional traits determine trade-offs and niches in a tropical forest community. Proc. Natl. Acad. Sci. 108 (51), 20627–20632.

Tan, Z.H., Wu, Z., Hughes, A.C., Schaefer, D., Zheng, J., Lan, G., Yang, C., Tao, Z., Chen, B., Tian, Y., Song, L., Jatoi, M.T., Zhao, J., Yang, L., 2017. On the ratio of intercellular to ambient CO_2 (c_i/c_a) derived from ecosystem flux. Int. J. Biometeorol. 61 (12), 2059–2071.

Tiwari, R., Gloor, E., da Cruz, W.J.A., Marimom, B.S., Marimon-Junio, B.H., Reis, S.M., Souza, I.A., Krause, H.G., Slot, M., Winter, K., Ashley, D., Béu, R.G., Borges, C.S., Cunha, M.D., Fauset, S., Ferreira, L.D.S., Gonçalves, M.D.A., Lopes, T.T., Marques, E. Q., Mendonça, N.G., Mendonça, N., G, Noleto, P.T., Oliveira, C.H.L., Oliveira, M.A., Pireda, S., Prestes, N.C.C.S., Santos, D.M., Santos, E.B., Silva, E.L.S., Souza, I.A., Souza, L.J., Vitória, A.P., Foyer, C., Galbraith, D.,, 2020. Photosynthetic quantum efficiency in south-eastern Amazonian trees may be already affected by climate change. Plant Cell Environ. 1–12.

Toledano-Thompson, T., Loría-Bastarrachea, M.I., Aguilar-Vega, M.J., 2005. Characterization of henequen cellulose microfibers treated with an epoxide and grafted with poly(acrylic acid). Carbohydr. Polym. 62 (1), 67–73.

Toubiana, D., Fernie, A.R., Nikoloski, Z., Fait, A., 2013. Network analysis: tackling complex data to study plant metabolism. Trends Biotechnol. 31 (1), 29–36.

Tng, D.Y., Apgaua, D.M., Ishida, Y.F., Mencuccini, M., Lloyd, J., Laurance, W.F., Laurance, S.G., 2018. Rainforest trees respond to drought by modifying their hydraulic architecture. Ecol. Evol. 8 (24), 12479–12491.

Tyree, M.T., Ewers, F.W., 1991. The hydraulic architecture of trees and other woody-plants. New Phytol. 119 (3), 345–360.

Tyree, M.T., Sperry, J.S., 1989. Vulnerability of xylem to cavitation and embolism. Annu. Rev. Plant. Physiol. Plant Mol. Biol. 40 (1), 19–38.
Van Der Sleen, P., Groenendijk, P., Vlam, M., Anten, N.P., Boom, A., Bongers, F., Pons, T. L., Terburg, G., Zuidema, P.A., 2015. No growth stimulation of tropical trees by 150 years of CO_2 fertilization but water-use efficiency increased. Nat. Geosci. 8 (1), 24–28.
Verbančič, J., Lunn, J.E., Stitt, M., Persson, S., 2018. Carbon supply and the regulation of cell wall synthesis. Mol. Plant 11 (1), 75–94.
Werden, L.K., Waring, B.G., Smith-Martin, C.M., Powers, J.S., 2017. Tropical dry forest trees and lianas differ in leaf economic spectrum traits but have overlapping water-use strategies. Tree Physiol. 38, 517–530.
Westbrook, J.A., Guilderson, T.P., Colinvaux, P.A., 2006. Annual growth rings in a sample of *Hymenaea courbaril*. IAWA Bull. 27 (2), 193–197.
Westoby, M., Wright, I.J., 2006. Land-plant ecology on the basis of functional traits. Trends Ecol. Evol. 21 (5), 261–268.
Williamson, G.B., Wiemann, M.C., Geaghan, J.P., 2012. Radial allocation in *Schizolobium parahyba*. Am. J. Bot. 99 (6), 1010–1019.
Würth, M.R., Peláez-Riedl, S., Wright, S.J., Körner, C., 2005. Non-structural carbohydrates pools in a tropical forest. Oecologia 143 (1), 11–24.
Yamada, T., Bork, P., 2009. Evolution of biomolecular networks – lessons from metabolic and protein interactions. Nat. Rev. Mol. Cell Biol. 10 (11), 791–803.
Zanne, A.E., Westoby, M., Falster, D.S., Ackerly, D.D., Loarie, S.R., Arnold, S.E., Coomes, D.A., 2010. Angiosperm wood structure: Global patterns in vessel anatomy and their relation to wood density and potential conductivity. Am. J. Bot. 97 (2), 207–215.
Zhang, T., Cao, Y., Chen, Y., Liu, G., 2015. Non-structural carbohydrate dynamics in *Robinia pseudoacacia* saplings under three levels of continuous drought stress. Trees 29 (6), 1837–1849.
Zhou, H., Chen, Y., Hao, X., Zhao, Y., Fang, G., Yang, Y., 2019. Tree rings: a key ecological indicator for reconstruction of groundwater depth in the lower Tarim River. Northwest China. Ecohydrology 12 (8), e2142.
Zuidema, P.A., 2015. Tropical forests in a changing world. Inaugural lecture of Professor of Tropical Forest Ecology, Wageningen University, 28 pg.
Zuidema, P.A., Poulter, B., Frank, D.C., 2018. A wood biology agenda to support global vegetation modelling. Trends Plant Sci. 23 (11), 1006–1015.
Zuidema, P.A., Baker, P.J., Groenendijk, P., Schippers, P., Van Der Sleen, P., Vlam, M., Sterck, F., 2013. Tropical forests and global change: Filling knowledge gaps. Trends Plant Sci. 18 (8), 413–419.
Zykwinska, A.W., Ralet, M., Garnier, C.D., Thibault, J.J., 2005. Evidence for in vitro binding of pectins side chains to cellulose. Plant Physiol. 139 (1), 397–407.